The Nucleus ***61***, *No. 2 (2024) 69-78*

https://doi.org/10.71330/thenucleus.2024.1397

www.thenucleuspak.org.pk

The Nucleus

ISSN 0029-5698 (Print)

ISSN 2306-6539 (Online)

Analysis and Optimization of Open Micro-Channel Heat Sink with Pin Fins by Modified Grey Relational Optimization

S.S. Raza, R. Bhushan*

Department of Physics, School of Science, YBN University, Ranchi, Jharkhand, India

ABSTRACT

This work successfully utilized grey relational optimization in conjunction with the standard deviation objective weighting approach to improve various response parameters in a microchannel heat sink with pin fins, including: the surface Nusselt number and total surface heat flux. Six process parameters were chosen for the simulation research of the open microchannel heat sink with pin fins based on the L-27 orthogonal array. These parameters are heat sink length (L), heat sink width (W), number of fins (N), fin height (a), base height (b) and fin thickness (d). The surface Nusselt number and total surface heat flux were selected as the output parameters. This work aids in understanding the effect of various parameters on the open microchannel heat sink with pin fins. The standard deviation objective weighting - grey relational optimization method optimized the process parameters. ANSYS Fluent software was utilized to simulate the entire open microchannel heat sink with pin fins according to the L-27 orthogonal array. The optimal configuration for the process parameters was determined to be a heat sink length of 80 mm, width of 100 mm, 5 fins, fin height of 30 mm, base height of 8 mm and fin thickness of 2 mm. Among these parameters, the number of fins was found to be the most influential factor, followed by base height, fin thickness, width of the heat sink, fin height, and length of the heat sink. The findings indicate that these parameters play a critical role in the thermal performance optimization of microchannel heat sinks.

Keywords: *Microchannel heat sink, Grey relational optimization, Surface heat flux, Surface Nusselt number, optimization*

1. Introduction

Electronic devices generate significant heat during operation. This heat needs efficient management to prevent overheating and ensure reliable performance. Micro-channel heat sinks (MCHS) with pin fins are a promising technology for thermal management due to their high surface area and efficient heat transfer capabilities. The movement toward smaller, more durable electronics has completely changed how consumers interact with technology in today's fast-paced market. Daily demand for miniaturization is rising across a wide range of devices from laptops and cellphones to automotive and medical equipment [1]. In today's rapidly evolving industry, the trend towards smaller and more durable electronic products is significantly changing how consumers interact with technology. This shift is evident in various sectors, including: smartphones, laptops, automotive systems and medical devices. The demand for the miniaturization is increasing as consumers seek more compact, robust and efficient devices that offer enhanced functionality and convenience. This trend towards smaller, more resilient technology is reshaping the design and manufacturing processes across multiple industries [2]. While technological advancements open up numerous opportunities, they also bring certain challenges. The significant miniaturization of energy systems and electronic devices requires the precise arrangement of complex components within a limited space. This compact design leads to higher densities of electronic components, which in turn generate substantial heat flow and create hot spots. Effective heat management becomes crucial to maintain the performance and longevity of modern electrical equipment. Without adequate cooling, these devices can overheat leading to reduced efficiency, potential failures, and shorter lifespans. The need for internal cooling systems in miniaturized devices is paramount. These cooling systems must be highly efficient and capable of dissipating heat effectively in a confined space. Engineers and designers are constantly innovating to develop advanced cooling solutions, such as: microchannel heat sinks, heat pipes, and phase-change materials. These technologies help manage the thermal load and ensure the reliable operation of electronic devices [3]. Microchannel heat sinks (MCHSs) have demonstrated significant potential for addressing these thermal management challenges. Researchers' attention has been drawn to microchannel heat sinks (MCHSs), a type of liquid-cooling heat sink that has replaced standard air-cooling heat sinks by exhibiting desirable performance in addition to compact design [4, 5]. Over time, extensive research has been conducted to enhance the hydrothermal performance of microchannel heat sinks (MCHS) by implementing various innovative strategies. These strategies include, modulating the pin-fin arrangements, altering fin shapes, adjusting fin spacing and fin tip clearance. Through these diverse approaches, researchers aim to optimize the design and operation of MCHS, ultimately achieving greater efficiency in thermal management for applications ranging from electronics cooling to industrial processes [6]. Technological developments bring about endless opportunities, but they also have drawbacks. An optimal arrangement of complex components within a limited space is essential for the aggressive miniaturization of energy systems and electronic devices [7]. This frequently raises the component's operating temperature and results in a notable increase in heat fluxes produced per unit volume [8]. Elevated temperatures have been linked to shorter lifespans, decreased efficiency and a higher chance of

*Corresponding author: raviroy76@gmail.com

component malfunction. Therefore, in order to ensure the consistent and reliable operation of these devices, it is imperative to evacuate the surplus heat effectively. The pursuit of developing a sophisticated cooling technique to address thermal management issues in electronic equipment has become increasingly consequential for engineers [9]. MCHSs have emerged as a highly effective solution for managing thermal imbalances and enhancing the performance of miniature systems. Their design and functionality offer significant advantages over traditional cooling methods, especially in applications where space is limited and efficient heat dissipation is critical [10]. Electronic devices generate significant heat during operation. This heat needs efficient management to prevent overheating and ensure reliable performance. MCHS with pin fins are a promising technology for thermal management due to their high surface area and efficient heat transfer capabilities [11]. In today's quickly changing market, the transition to smaller and more durable electronic items has altered how customers interact with technology. Whether it's smartphones, computers, automotive systems or medical gadgets, the desire for downsizing is always expanding [12]. While technological advancements create numerous opportunities, they also come with certain challenges. The growing downsizing of energy systems and electronic gadgets involves the careful grouping of complicated components inside a limited space[13]. The functionality of contemporary electrical equipment depends on efficient heat management. Internal cooling systems are required because to the rapid heat flow and hot spots caused by the high-density integration of electronic components [2]. These advanced cooling devices are designed to efficiently manage heat in compact electronic systems where space and cooling efficiency are critical [14]. Microchannel heat sinks represent a significant advancement over traditional air-cooling heat sinks. Unlike their air-cooled counterparts, which rely on air flow to dissipate heat, MCHSs utilize liquid cooling. This shift from air to liquid cooling is driven by the superior thermal conductivity of liquids, which allows MCHSs to achieve more effective heat removal in a smaller footprint. Researchers have increasingly focused on MCHSs due to their ability to handle high thermal loads while maintaining a compact and lightweight design. This makes them particularly suitable for applications in modern electronics, where devices are becoming more powerful and densely packed. Their small size and efficient heat transfer capabilities make them ideal for use in environments with limited space, such as in high-performance computing systems, aerospace applications, and compact consumer electronics. Traditionally, experienced technicians chose parameters by trial and error, which was time and money intensive for each new welded product to match the specified requirements of the welded joint. Several researchers have used single-quality characteristic analyses to overcome these difficulties. The single-objective approach consists entirely of simplifications of the genuine situation. Open micro-channel heat sink with pin fins processes the heat sink's length, breadth, number of fins, fin height, base height, and fin thickness to maximize heat transmission. All of these process factors have the potential to alter the quality and attributes of the weld. It is difficult to discover the ideal design of open micro-channel heat sink with pin fins process parameters by employing single objective optimization approaches such as ANOVA [15], response surface optimization [16], Taguchi method [7], thus, the total heat transfer rate is represented by many quality characteristics. To improve welding characteristics under ideal process circumstances, it is necessary to investigate the multi-objective optimization strategy. Then, using grey relational analysis (GRA), a correlation between the process's quality attributes in these situations is established [17, 18].

While previous studies have focused on optimizing various aspects of MCHS with pin fins, this research introduces a novel approach by integrating the standard deviation objective weighting method with the GRA-based Taguchi method. This combination allows for a comprehensive multi-objective optimization that has not been systematically explored in the literature. Many researchers have concentrated on optimizing open microchannel heat sinks with pin fins, recognizing their importance in enhancing thermal performance and efficiency in compact systems. These optimizations typically aim to balance various factors, such as heat dissipation efficiency and structural design, to achieve optimal performance. However, despite the extensive research in this area, there has been a notable lack of systematic studies that combine specific optimization techniques for comprehensive multi-objective analysis. Specifically, there has not been a detailed integration of the standard deviation objective weighting method with the GRA-based Taguchi method for optimizing open microchannel heat sinks with pin fins. The standard deviation objective weighting method is a technique used to assign weights to different response variables based on their variability. This method helps prioritize responses with higher variability or greater significance, ensuring that the optimization process accounts for the most critical performance metrics. In the context of heat sinks, this might involve weighting factors such as: thermal performance, reliability and cost. In this paper, we investigate the use of both the standard deviation objective weighting approach and the GRA-based Taguchi method to solve multi-criteria optimization problems in open microchannel heat sinks with pin fins. By combining these technologies, we hope to improve important performance metrics including: total surface heat flow and the Nusselt number.

2. Numerical Analysis

The open microchannel heat sinks with pin fins were numerically analyzed using ANSYS Fluent 24.0. The following are the governing equations for every element in the finite element formulation: The equation 1 for momentum conservation is as follows:

$$\rho\vec{\psi}\cdot\nabla\vec{v} = \mu\nabla^2\vec{v} - \nabla P \quad (1)$$

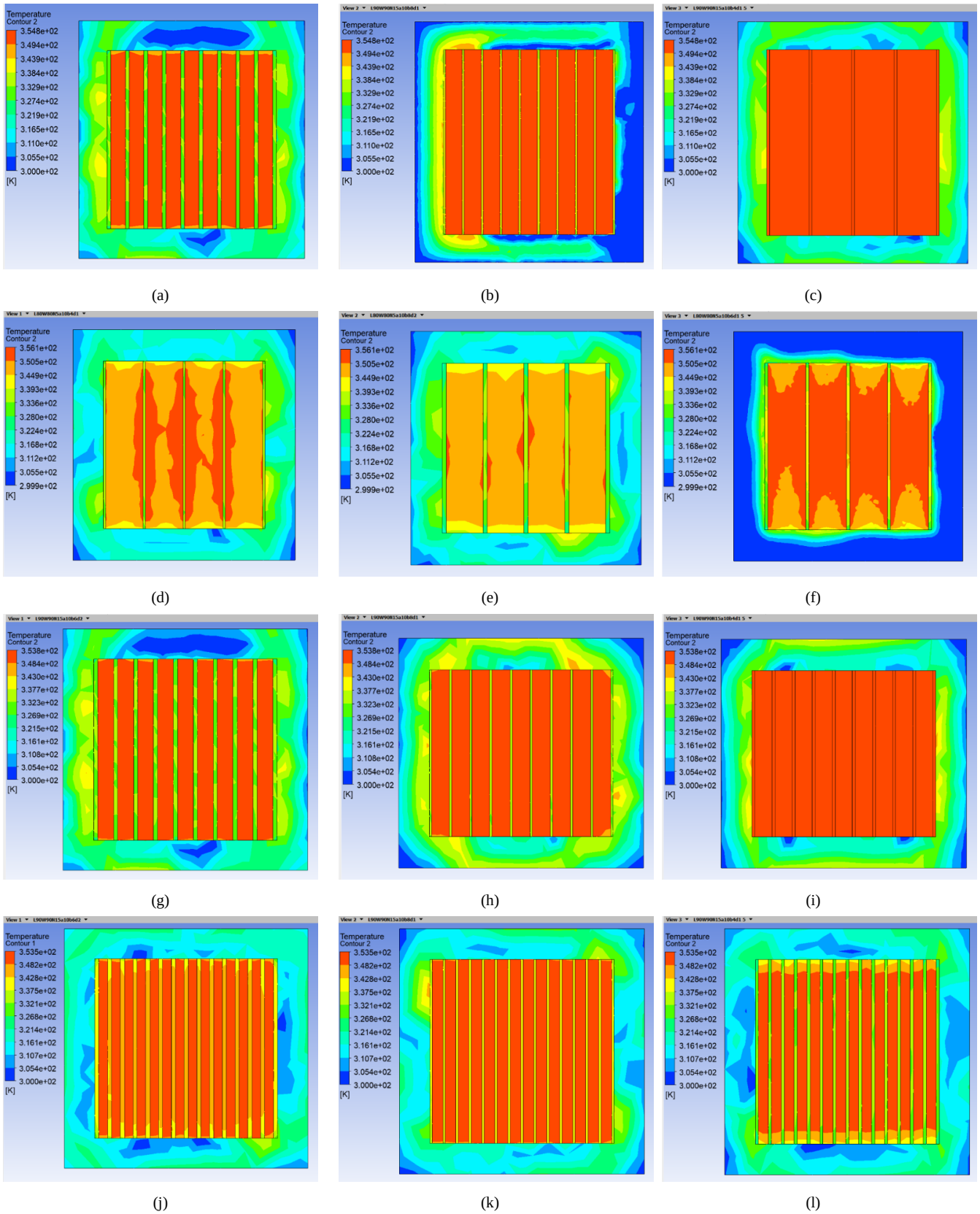

Fig. 1. Temperature Contours (a) - L90W90N15a10b4d1.5, (b) - L90W90N15a10b6d2, (c) - L90W90N15a10b8d1, (d) - L80W80N5a10b4d1, (e) - L80W80N5a10b8d2, (f) - L80W80N5a10b6d1.5, (g) - L90W80N10a30b4d1.5, (h) - L90W80N10a30b6d2, (i) - L90W80N10a30b8d1

Equation 2 for mass conservation or continuity is provided as:

$$\nabla \cdot (\rho \vec{v}) = 0 \quad (2)$$

Here, "ρ" is the density of the fluid and "υ" is the velocity vector of the flow field.

Energy conservation equation 3 for fluid is given as:

$$\rho C_p \nabla \cdot (\vec{v} T) = k_f \nabla^2 T \quad (3)$$

The energy conservation equation 4 for the solid is expressed as:

$$\nabla^2 T = 0 \quad (4)$$

Table 1. Properties of working fluids

	ρ (kg/m^3)	C_p (J/kgK)	μ (pa.s)
Air	998	4182	0.001

Numerical simulations are done for 27 cases as orthogonal array of different geometrical arrangements as per Table 2. Total surface heat flux and surface Nusselt number has been evaluated on fluent and tabulated on Table 3

2.1 Design of Experiment (DOE)

In this study, length of the heat sink (L), Width of the heat sink (W), No of fins (N), Fin height (a), Base height (b), and Fin thickness (d) were selected as process parameters of the open micro-channel heat sink with pin fins. Table 2 displays these process parameters together with their respective levels. As a result, 729 combinations of 3 × 3 × 3 × 3× 3× 3 were taken into account. But only nine combinations of the samples could produce findings with the same level of confidence as if they were taken into consideration individually, according to Taguchi's L-27 orthogonal array [32]. A Taguchi orthogonal array was made using Minitab-23's design of the experiment approach, and Table 3 displays the DOE.

Table 2: Process parameters and their levels

Parameters	Level 1	Level 2	Level 3
Length of the heat sink (L), mm	80	90	100
Width of theheat sink (W), mm	80	90	100
No of fins (N)	5	10	15
Fin height (a), mm	10	20	30
Base height (b), mm	4	6	8
Fin thickness (d), mm	1	1.5	2

3. Standard Deviation Objective Weighting Method

The standard deviation objective weighting method is a technique used in multi-objective optimization to determine the relative importance of various objectives based on their variability. This method assigns weights to different objectives by evaluating their standard deviations, thus allowing for a balanced consideration of their impact on the overall optimization process. Each criterion's weight (w_j) was evaluated using the standard deviation objective weighing technique [19, 20]. This method provides a structured approach to multi-objective optimization by focusing on the relative importance of each objective based on its variability. This method facilitates a balanced and effective optimization strategy, leading to more robust and well-considered solutions. The performance defining criteria (PDC) are crucial in evaluating and optimizing various response variables in a multi-objective optimization problem. These criteria are derived based on the weights assigned to each response, reflecting their relative importance. The process involves several detailed steps to ensure accurate and balanced assessment of performance metrics. The PDC for each response were derived using their weight. The first step is to create a preliminary decision matrix with six process parameters and 27 simulations. Next, using Equation 5, the decision matrix is normalized following the computation of the best and worst values for each process parameter.

Table 3. Design of Experiment according to L-27 orthogonal array

S.No.	Length of the heat sink (L)	Width of the heat sink (W)	No of fins (N)	Fin height (a)	Base height (b)	Fin thickness (d)
1	80	80	5	10	4	1
2	80	80	5	10	6	1.5
3	80	80	5	10	8	2
4	80	90	10	20	4	1
5	80	90	10	20	6	1.5
6	80	90	10	20	8	2
7	80	100	15	30	4	1
8	80	100	15	30	6	1.5
9	80	100	15	30	8	2
10	90	80	10	30	4	1.5
11	90	80	10	30	6	2
12	90	80	10	30	8	1
13	90	90	15	10	4	1.5
14	90	90	15	10	6	2
15	90	90	15	10	8	1
16	90	100	5	20	4	1.5
17	90	100	5	20	6	2
18	90	100	5	20	8	1
19	100	80	15	20	4	2
20	100	80	15	20	6	1
21	100	80	15	20	8	1.5
22	100	90	5	30	4	2
23	100	90	5	30	6	1
24	100	90	5	30	8	1.5
25	100	100	10	10	4	2
26	100	100	10	10	6	1
27	100	100	10	10	8	1.5

$$X_{ij}^{+} = \frac{X_{ij} - X_j^{\text{worst}}}{X_j^{\text{best}} - X_j^{\text{worst}}} \quad (5)$$

Where X_{ij}^{+} represents the normalized value of the i[th] design for the j[th] response. Correlation and standard deviation coefficients were calculated using Minitab 24. These coefficients were then employed to evaluate information production. The weight (ξ_j) for each condition was subsequently calculated using Equation 3. Table 3 illustrates that the PDC for all responses were established based on these weights.

$$\xi_j = \frac{c_j}{\sum_{k=1}^{m} c_j} \quad (6)$$

where, $\xi_j \geq 0$ and $\sum_{k=1}^{m} c_j = 1$

Table 3: Performance Defining Criteria (PDCs)

S. #	Performance-defining criteria (PDC)			Impact on PDC
1	Total Surface Heat Flux [W/m^2]	0.5	PDC-1	Higher the better
2	Surface Nusselt Number (Nu)	0.5	PDC-2	Higher the better

4. Hybrid Gray Relational Methodology

4.1 S/N ration

The signal-to-noise (S/N) ratio is a critical metric in optimization, particularly within the context of robust design and quality engineering. It is extensively used in the Taguchi method for experimental design to improve the quality and performance of products and processes by minimizing the effects of uncontrollable variability. Based on their characteristics, three types of S/N ratios are used: smaller-the-better, larger-the-better and nominal-the-best. In this study, total surface heat flux and surface Nusselt number are considered, with higher values being preferred. There are three main types of S/N ratios used in optimization, each suited for different types of response variables:

SN ratio for “lager is better”

$$SN_L = -10log(\frac{1}{n}\sum_{i=1}^{n}\frac{1}{y^{i^2}} \quad (7)$$

SNs ratio for "smaller is better"

$$SN_s = -10log\sum_{i=1}^{n} y^{i^2} \quad (8)$$

SN_n ratio for "nominal is better"

$$SN_n = 10\log 10\ (Square of\ mean / variance) \quad (9)$$

4.2 Normalisation of S/N ratio

Normalization is necessary to bring different units and scales of the criteria to a comparable level. The normalization formula depends on the type of criterion.

Larger-the-better

$$y_i^{*}(m) = \frac{y_i(m) - \min y_i(m)}{\max y_i(m) - \min y_i(m)} \quad (10)$$

$$y_i^{*}(m) = \frac{\max y_i(m) - y_i(m)}{\max y_i(m) - \min y_i(m)} \quad (11)$$

For nominal, the better for

$$y_i^{*}(m) = \frac{1 - / y_i(m) - y_0 b(m) /}{\max y_i(m) - y_0 b(m)} \quad (12)$$

4.3 Deviation sequence

The deviation sequence can be represented as [9]

$$\Delta_{0i}(k) = \left| y_0^{*}(m) - y_k^{*}(m) \right| \quad (13)$$

4.4 Calculate the Grey Relational Coefficient (GRC)

The GRC quantifies the relationship between the ideal (best) and actual normalized values. It is calculated using the formula:[21]

$$\xi_{ij} = \frac{\Delta_{min} + \zeta\Delta_{max}}{\Delta_{ij} + \zeta\Delta_{max}} \quad (14)$$

ξ_{ij} is the GRC for the i[th] criterion and j[th] alternative.

4.5 Compute the Grey Relational Grade (GRG)

The GRG aggregates the GRCs to provide an overall performance score for each alternative. It is computed using [21].

$$\gamma_i = \frac{1}{n}\sum_{k=1}^{n}\xi_i(k) \quad (15)$$

5. Optimization using GRA method

The simulations were performed using the L-27 orthogonal array. Figure 2 shows graphs of total surface heat flux. Table 4 displays the total surface heat flux and surface Nusselt number recorded for all 27 simulation sets.

Equation 10 was used to obtain the normalized S/N ratio for total surface heat flux, and Table 5 displays the surface Nusselt number.

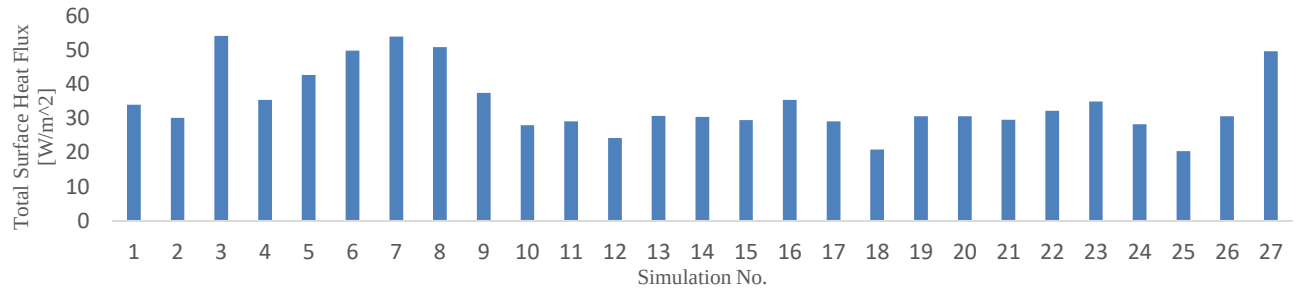

Fig. 2 (a) Total surface heat flux plot for all experiments

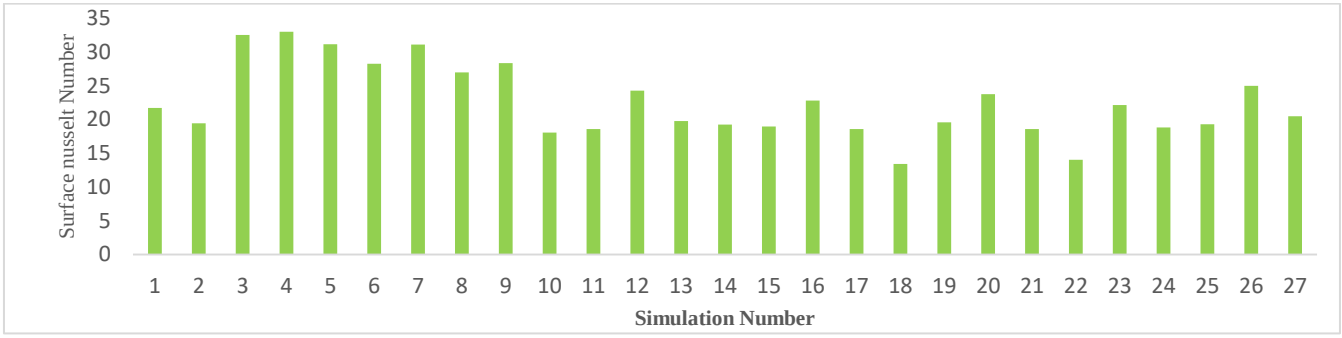

Fig. 2 (b) Surface Nusselt Number for all experiment

Table 4: Simulation Results

	Input Process Parameters						Response	
S. No.	Length of the heat sink (L)	Width of the heat sink (W)	No of fins (N)	Fin height (a)	Base height (b)	Fin thickness (d)	Total Surface Heat Flux [W/m^2]	Surface Nusselt Number
1	80	80	5	10	4	1	33.95096	21.72327
2	80	80	5	10	6	1.5	30.1703	19.40953
3	80	80	5	10	8	2	54.15893	32.53679
4	80	90	10	20	4	1	35.3542	32.97963
5	80	90	10	20	6	1.5	42.72831	31.12578
6	80	90	10	20	8	2	49.84818	28.23629
7	80	100	15	30	4	1	53.91737	31.11047
8	80	100	15	30	6	1.5	50.86978	26.96261
9	80	100	15	30	8	2	37.41472	28.3549
10	90	80	10	30	4	1.5	28.00394	18.06982
11	90	80	10	30	6	2	29.11692	18.58572
12	90	80	10	30	8	1	24.28777	24.28777
13	90	90	15	10	4	1.5	30.73066	19.74369
14	90	90	15	10	6	2	30.41855	19.25404
15	90	90	15	10	8	1	29.49225	18.93596
16	90	100	5	20	4	1.5	35.42092	22.80109
17	90	100	5	20	6	2	29.11692	18.58572
18	90	100	5	20	8	1	20.90134	13.41547
19	100	80	15	20	4	2	30.59097	19.55782
20	100	80	15	20	6	1	30.59679	23.76713
21	100	80	15	20	8	1.5	29.58593	18.58089
22	100	90	5	30	4	2	32.25954	14.00099
23	100	90	5	30	6	1	34.93172	22.12668
24	100	90	5	30	8	1.5	28.32795	18.79545
25	100	100	10	10	4	2	20.45325	19.30592
26	100	100	10	10	6	1	30.6277	24.99635
27	100	100	10	10	8	1.5	49.61141	20.47484

Table 5: Normalise S/N ratio of response.

S. No.	Length of the heat sink (L)	Width of the heat sink (W)	No of fins (N)	Fin height (a)	Base height (b)	Fin thickness (d)	Normalize Total Surface Heat Flux	Normalize Surface Nusselt Number
1	80	80	5	10	4	1	0.400458	0.575356
2	80	80	5	10	6	1.5	0.288291	0.69362
3	80	80	5	10	8	2	1	0.022635
4	80	90	10	20	4	1	0.44209	0
5	80	90	10	20	6	1.5	0.66087	0.094758
6	80	90	10	20	8	2	0.872106	0.24245
7	80	100	15	30	4	1	0.992833	0.09554
8	80	100	15	30	6	1.5	0.902416	0.307553
9	80	100	15	30	8	2	0.503223	0.236388
10	90	80	10	30	4	1.5	0.224018	0.762098
11	90	80	10	30	6	2	0.257039	0.735729
12	90	80	10	30	8	1	0.113765	0.444275
13	90	90	15	10	4	1.5	0.304916	0.67654
14	90	90	15	10	6	2	0.295656	0.701568
15	90	90	15	10	8	1	0.268174	0.717826
16	90	100	5	20	4	1.5	0.44407	0.520265
17	90	100	5	20	6	2	0.257039	0.735729
18	90	100	5	20	8	1	0.013294	1
19	100	80	15	20	4	2	0.300772	0.686041
20	100	80	15	20	6	1	0.300945	0.470887
21	100	80	15	20	8	1.5	0.270954	0.735976
22	100	90	5	30	4	2	0.350276	0.970072
23	100	90	5	30	6	1	0.429556	0.554736
24	100	90	5	30	8	1.5	0.233631	0.725008
25	100	100	10	10	4	2	0	0.698916
26	100	100	10	10	6	1	0.301862	0.408057
27	100	100	10	10	8	1.5	0.865081	0.639168

The GRC was calculated using Equation 14. This coefficient quantifies the degree of similarity between the ideal (or reference) solution and the actual data for each response variable. To compute the GRC, the deviations between the reference values and the observed values are first assessed. The weight for each response, denoted as (ξ), was obtained from Table 3. These weights were determined using the standard deviation objective weighting method, which evaluates the relative importance of each response based on its variability. The calculated weights are detailed in Table 7, reflecting the contribution of each response to the overall optimization process.

The GRG for each alternative was calculated using Equation 15. This calculation involves aggregating the GRCs for each response variable to derive an overall performance score for each alternative. The GRG provides a comprehensive measure of how closely each alternative aligns with the ideal solution across all criteria. The results of these calculations, including the GRG values and their corresponding rankings, are presented in Table 8. This table summarizes the performance scores for each alternative, allowing for a clear comparison and ranking based on the aggregated Grey Relational Grades.

The mean GRC for the length of the heat sink, spanning stages 1 to 9, was calculated by averaging the GRC values from three simulation ranges: simulations 1 to 9, 9 to 18, and 18 to 27. The results are presented in Table 9, which displays the GRA grade responses. This table provides a detailed view of the GRC averages and their implications for the optimization process.

Table 6 displays the deviation sequence, which was calculated for each simulation attempt using equation 13.

Table 6: The deviation sequences for all experiments

Exp. No.	$\Delta_{0i}(1)$	$\Delta_{0i}(2)$
1	0.599542	0.424644
2	0.711709	0.30638
3	0	0.977365
4	0.55791	1
5	0.33913	0.905242
6	0.127894	0.75755
7	0.007167	0.90446
8	0.097584	0.692447
9	0.496777	0.763612
10	0.775982	0.237902
11	0.742961	0.264271
12	0.886235	0.555725
13	0.695084	0.32346
14	0.704344	0.298432
15	0.731826	0.282174
16	0.55593	0.479735
17	0.742961	0.264271
18	0.986706	0
19	0.699228	0.313959
20	0.699055	0.529113
21	0.729046	0.264024
22	0.649724	0.029928
23	0.570444	0.445264
24	0.766369	0.274992
25	1	0.301084
26	0.698138	0.591943
27	0.134919	0.360832
ξ	0.5	0.5

Table 7: Grey Relational Coefficient for the response.

Exp. No.	GRC for Surface Heat Flux	GRC for Surface Nusselt Number
1	0.454734765	0.540748929
2	0.412640362	0.620055445
3	1	0.338440467
4	0.472630033	0.333333333
5	0.595854944	0.35581055
6	0.79631315	0.397598639
7	0.985869119	0.356008727
8	0.836701929	0.419305897
9	0.501616615	0.395691079
10	0.391855168	0.677597031
11	0.402265198	0.654218044
12	0.360689157	0.473608033
13	0.418380679	0.60719425
14	0.415163928	0.626227558
15	0.405901623	0.639244229
16	0.473516066	0.510341937
17	0.402265198	0.654218044
18	0.336313989	1
19	0.41693488	0.614281306
20	0.416994913	0.485855222
21	0.40681951	0.654429336
22	0.434886939	0.943523635
23	0.467095826	0.528952856
24	0.394829651	0.64516831
25	0.333333333	0.624154659
26	0.417314045	0.457899176
27	0.787502597	0.580833614

Table 8: The calculated Grey relational grade and its order

S. No.	Length of the heat sink (L)	Width of the heat sink (W)	No of fins (N)	Fin height (a)	Base height (b)	Fin thickness (d)	GRG	Rank
1	80	80	5	10	4	1	0.497742	19
2	80	80	5	10	6	1.5	0.516348	15
3	80	80	5	10	8	2	0.66922	4
4	80	90	10	20	4	1	0.402982	27
5	80	90	10	20	6	1.5	0.475833	22
6	80	90	10	20	8	2	0.596956	7
7	80	100	15	30	4	1	0.670939	3
8	80	100	15	30	6	1.5	0.628004	6
9	80	100	15	30	8	2	0.448654	24
10	90	80	10	30	4	1.5	0.534726	8
11	90	80	10	30	6	2	0.528242	10
12	90	80	10	30	8	1	0.417149	26
13	90	90	15	10	4	1.5	0.512787	17
14	90	90	15	10	6	2	0.520696	13
15	90	90	15	10	8	1	0.522573	12
16	90	100	5	20	4	1.5	0.491929	20
17	90	100	5	20	6	2	0.528242	10
18	90	100	5	20	8	1	0.668157	5

19	100	80	15	20	4	2	0.515608	16
20	100	80	15	20	6	1	0.451425	23
21	100	80	15	20	8	1.5	0.530624	9
22	100	90	5	30	4	2	0.689205	1
23	100	90	5	30	6	1	0.498024	18
24	100	90	5	30	8	1.5	0.519999	14
25	100	100	10	10	4	2	0.478744	21
26	100	100	10	10	6	1	0.437607	25
27	100	100	10	10	8	1.5	0.684168	2

The significance of each factor in influencing the GRG was determined by ranking the process parameters. The ranking is as follows: Number of fins > base height > fin thickness > width of the heat sink > fin height > length of the heat sink. This ranking indicates that the number of fins plays the most crucial role in the overall performance of the microchannel pin fins. Figure 3 illustrates the main effects plot of the GRG, generated using Minitab 19. This plot visually represents the impact of each process parameter on the GRG. According to the analysis, the optimal process parameters are A1B3C1D3E3F3, which correspond to a heat sink length of 80 mm, a width of 100 mm, 5 fins, a fin height of 30 mm, a base height of 8 mm, and a fin thickness of 2 mm. These settings yield the best performance for the microchannel heat sink with pin fins, as identified by the GRG analysis.

Table 9: Responses for the GRA Grade

Sr. No	Laser welding process parameters	Grey relational grade			Main effect (Max-Min)	Rank	Mean
		Level 1	Level 2	Level 3			
1	A(Length of the heat sink)	0.545186	0.524944	0.533934	0.02024188	6	0.534688
2	B (Width of the heat sink)	0.517898	0.526562	0.559605	0.04170657	4	0.534688
3	C (No of fins)	0.564318	0.506267	0.533479	0.05805121	1	0.534688
4	D (Fin height)	0.537765	0.517973	0.548327	0.03035401	5	0.534688
5	E (Base height)	0.53274	0.50938	0.561944	0.05256449	2	0.534688
6	F (Fin thickness)	0.5074	0.543824	0.552841	0.04544104	3	0.534688

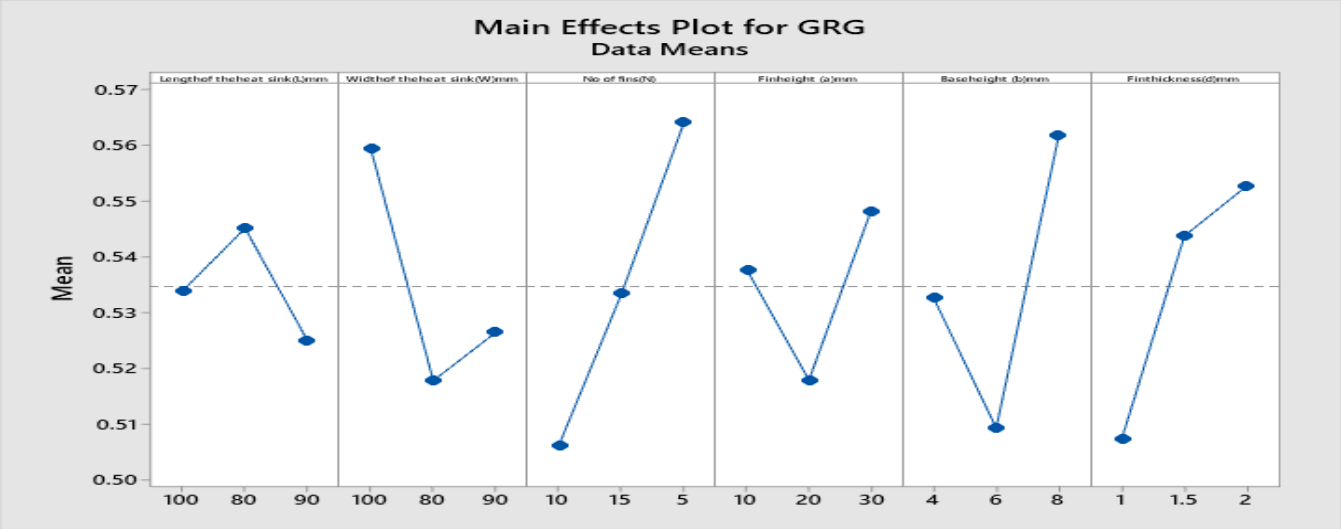

Fig. 3. Main effects plot for GRG.

6. Conclusion

This study effectively utilized the standard deviation objective weighting approach combined with grey relational optimization to optimize multiple responses, including total surface heat flux and surface Nusselt number. The analysis revealed that the optimal process parameters for achieving the best performance were identified as A1B3C1D3E3F3. Specifically, these parameters correspond to a heat sink length of 80 mm, a heat sink width of 100 mm, 5 fins, a fin height of 30 mm, a base height of 8 mm, and a fin thickness of 2 mm. The number of fins is a crucial factor in the performance of a microchannel heat sink with pin fins. It has the most significant impact on heat dissipation efficiency, followed by the base height, fin thickness, width of the heat sink, fin height, and length of the heat sink. The length of the heat sink has the most substantial impact on surface heat flux, accounting for 44.65% of the variance. This is followed by the width of the heat sink, which contributes 3.46%, fin

thickness at 2.37%, number of fins at 1.42%, base height at 1.28%, and fin height, which has the least impact at only 0.54%. Length of the heat sink affects the Nusselt number maximum 55.31 % followed by no of pin fins 9.13 %, fin thickness 2.60 %, fin height 1.18 %, width of the heat sinks 0.81 %, base height has minimum affect only 0.24%. It is observed that the optimum value for total surface heat flux are length of the heat sink 80 mm, width of the heat sink 100 mm, no of fins 10, fin height 20 mm, base height 6 mm and fin thickness 1 mm.

List of Abbrevations

Abbreviation	Full Term
MCHS	Microchannel Heat Sink
GRA	Grey Relational Analysis
SDOW	Standard Deviation Objective Weighting
Nusselt Number	A dimensionless number representing the ratio of convective to conductive heat transfer
ANOVA	Analysis of Variance
L-27	Orthogonal Array Design with 27 Experimental Runs
W	Heat Sink Width
L	Heat Sink Length
N	Number of Fins
a	Fin Height
b	Base Height
d	Fin Thickness

References

[1] H.A. Mohammed, P. Gunnasegaran, and N.H. Shuaib, "Influence of channel shape on the thermal and hydraulic performance of microchannel heat sink," *Int. Commun. Heat Mass Transf.*, vol. 38, no. 4, pp. 474–480, 2011.

[2] Y. Xie, T.U.K.Nutakki, D. Wang, X. Xu, Y. Li., M.N. Khan, and R. Chen "Multi-objective optimization of a microchannel heat sink with a novel channel arrangement using artificial neural network and genetic algorithm," *Case Stud. Therm. Eng.*, vol. 53, no. September 2023, 2024

[3] Y. Wang, M. Lou, Y. Wang, C. Fan, C. Tian, and X. Qi, "Experimental investigation of the effect of rotation rate and current speed on the dynamic response of riserless rotating drill string," *Ocean Eng.*, vol. 280, pp. 114542, 2023.

[4] D. Jung, H. Lee, D. Kong, E. Cho, K. Jung, C R. Kharangate, M. Iyengar [e], C. Malone, M. Asheghi, K. E. Goodson, and H. Lee, "Thermal design and management of micro-pin fin heat sinks for energy-efficient three-dimensional stacked integrated circuits," *Int. J. Heat Mass Transf.*, vol. 175, pp. 121192, 2021.

[5] R. Moosavi, M. Banihashemi, C.-X. Lin, and P.-Y. Abel Chuang, "Combined effects of a microchannel with porous media and transverse vortex generators (TVG) on convective heat transfer performance," *Int. J. Therm. Sci.*, vol. 166, pp. 106961, 2021.

[6] M.K. Mohit and R. Gupta, "Numerical investigation of the performance of rectangular micro-channel equipped with micro-pin-fin," *Case Stud. Therm. Eng.*, vol. 32, no. October 2021, pp. 101884, 2022.

[7] L.K. Pan, C.C. Wang, Y.C. Hsiao, and K.C. Ho, "Optimization of Nd:YAG laser welding onto magnesium alloy via Taguchi analysis," *Opt. Laser Technol.*, vol. 37, no. 1, pp. 33–42, 2005.

[8] A.G. Paleocrassas and J.F. Tu, "Low-speed laser welding of aluminum alloy 7075-T6 using a 300-W, single-mode, ytterbium fiber laser," *Weld. J. (Miami, Fla)*, vol. 86, no. 6, pp. 179–186, 2007.

[9] A.N. Haq, P. Marimuthu, and R. Jeyapaul, "Multi response optimization of machining parameters of drilling Al/SiC metal matrix composite using grey relational analysis in the Taguchi method," *Int. J. Adv. Manuf. Technol.*, vol. 37, no. 3–4, pp. 250–255, 2008.

[10] P. Bhandari, K.S. Rawat, Y.K. Prajapati, D. Padalia, L. Ranakoti, and T. Singh, "Design modifications in micro pin fin configuration of microchannel heat sink for single phase liquid flow: A review," *J. Energy Storage*, vol. 66, no. November 2022, pp. 107548, 2023.

[11] M. Harris, H. Wu, W. Zhang, and A. Angelopoulou, "Overview of recent trends in microchannels for heat transfer and thermal management applications," *Chem. Eng. Process. - Process Intensif.*, vol. 181, no. May, pp. 109155, 2022.

[12] M. Tabatabaei Malazi, K. Kaya, and A.S. Dalkılıç, "A computational case study on the thermal performance of a rectangular microchannel having circular pin-fins," *Case Stud. Therm. Eng.*, vol. 49, no. June, pp. 103111, 2023.

[13] A. Ravanji, A. Lee, J. Mohammadpour, and S. Cheng, "Critical review on thermohydraulic performance enhancement in channel flows: A comparative study of pin fins," *Renew. Sustain. Energy Rev.*, vol. 188, no. October, pp. 113793, 2023.

[14] Y. Pan, R. Zhao, Y. Nian, and W. Cheng, "Study on the flow and heat transfer characteristics of pin-fin manifold microchannel heat sink," *Int. J. Heat Mass Transf.*, vol. 183, pp. 122052, 2022.

[15] N.K. Singh, S. Balaguru, R.K. Rathore, A.K. Namdeo, and A. Kaimkuriya, "Multi-Criteria Decision-Making Technique for Optimal Material Selection of AA7075/SiC Composite Foam using COPRAS Technique," *J. Mines, Met. Fuels*, vol. 71, no. 10, pp. 1374–1379, 2023.

[16] Y. Koli, N. Yuvaraj, S. Aravindan, and Vipin, "Multi-response mathematical model for optimization of process parameters in CMT welding of dissimilar thickness AA6061-T6 and AA6082-T6 alloys using RSM-GRA coupled with PCA," *Adv. Ind. Manuf. Eng.*, vol. 2, no. April, pp. 100050, 2021.

[17] S.V. Gosavi and M.D.Jaybhaye, "Friction stir welding process optimization of Al 7075/SiC composites using grey relational analysis," *Mater. Today Proc.*, vol. 72, pp. 719–723, 2023.

[18] M.P. Prabakaran and G.R. Kannan, "Optimization of laser welding process parameters in dissimilar joint of stainless steel AISI316/AISI1018 low carbon steel to attain the maximum level of mechanical properties through PWHT," *Opt. Laser Technol.*, vol. 112, no. October 2018, pp. 314–322, 2019.

[19] Y. Xu and Z. Cai, "Standard deviation method for determining the weights of group multiple attribute decision making under uncertain linguistic environment," *Proc. World Congr. Intell. Control Autom.*, no. July, pp. 8311–8316, 2008.

[20] R. Sharma, M.K. Pradhan, and P. Jain, "Optimal selection of an AA8011 reinforced nano Si3N4 composite using multi criteria decision-making method," *Mater. Today Proc.*, vol. 56, pp. 1399–1405, 2022.

[21] D. Deng, T. Li, Z. Huang, H. Jiang, S. Yang, and Y. Zhang, "Multi-response optimization of laser cladding for TiC particle reinforced Fe matrix composite based on Taguchi method and grey relational analysis," *Opt. Laser Technol.*, vol. 153, no. April, pp. 108259, 2022.